THYROID
Volume 33, Number 10, 2023

DOI: 10.1089/thy.2023.0201

Open camera or QR reader and scan code to access this article and other resources online.

Combination *BRAF*^{V600E} Inhibition with the Multitargeting Tyrosine Kinase Inhibitor Axitinib Shows Additive Anticancer Activity in *BRAF*^{V600E}-Mutant Anaplastic Thyroid Cancer

Viswanath Gunda,[1,*] Chandrayee Ghosh,[1,*] Jiangnan Hu,[1] Lisa Zhang,[2] Ya qin Zhang,[3] Min Shen,[3] and Electron Kebebew[1,4]

Background: Anaplastic thyroid cancer (ATC) is uniformly lethal. *BRAF*^{V600E} mutation is present in 45% of patients with ATC. Targeted therapy with combined BRAF and MEK inhibition in *BRAF*^{V600E}-mutant ATC can be effective, but acquired resistance is common because this combination targets the same pathway. Drug matrix screening, in *BRAF*^{V600E} ATC cells, of highly active compounds in combination with BRAF inhibition showed multitargeting tyrosine kinase inhibitors (MTKIs) had the highest synergistic/additive activity. Thus, we hypothesized that the combination of *BRAF*^{V600E} inhibition and an MTKI is more effective than a single drug or combined BRAF and MEK inhibition in *BRAF*^{V600E}-mutant ATC. We evaluated the effect of *BRAF*^{V600E} inhibitors in combination with the MTKI axitinib and its mechanism(s) of action.
Methods: We evaluated the effects of *BRAF*^{V600E} inhibitors and axitinib alone and in combination in *in vitro* and *in vivo* models of *BRAF*^{V600E}-mutant and wild-type ATC.
Results: The combination of axitinib and *BRAF*^{V600E} inhibitors (dabrafenib and PLX4720) showed an additive effect on inhibiting cell proliferation based on the Chou–Talalay algorithm in *BRAF*^{V600E}-mutant ATC cell lines. This combination also significantly inhibited cell invasion and migration ($p < 0.001$) compared with the control. Dabrafenib and PLX4720 arrested ATC cells in the G0/G1 phase. Axitinib arrested ATC cells in the G2/M phase by decreasing phosphorylation of aurora kinase B (Thr232) and histone H3 (Ser10) proteins and by upregulating the c-JUN signaling pathway. The combination of BRAF inhibition and axitinib significantly inhibited tumor growth and was associated with improved survival in an orthotopic ATC model.
Conclusions: The novel combination of axitinib and *BRAF*^{V600E} inhibition enhanced anticancer activity in *in vitro* and *in vivo* models of *BRAF*^{V600E}-mutant ATC. This combination may have clinical utility in *BRAF*^{V600E}-mutant ATC that is refractory to current standard therapy, namely combined BRAF and MEK inhibition.

Keywords: combination treatment, targeted therapy, axitinib, BRAF mutation, aurorakinase B, anaplastic thyroid cancer

Introduction

Anaplastic thyroid cancer (ATC) is one of the most aggressive human malignancies, with a median survival of 6 months in most patients.[1] Although ATC accounts for <2% of all thyroid cancer cases, it accounts for 40% of thyroid cancer deaths due to its aggressive nature and limited therapeutic options.[2] Surgical resection with radiation therapy and chemotherapy have limited effects on survival.[3] The *BRAF*^{V600E} mutation in patients with ATC is common (about

[1]Department of Surgery, Stanford University, Stanford, California, USA.
[2]Eunice Kennedy Shriver National Institute of Child Health and Human Development, National Institutes of Health, Bethesda, Maryland, USA.
[3]National Center for Advancing Translational Sciences, National Institutes of Health, Bethesda, Maryland, USA.
[4]Stanford Cancer Institute, Stanford University, Stanford, California, USA.
*Both these authors contributed equally as first authors.

45%)[4,5] and is associated with more aggressive disease and a higher mortality rate when it occurs with a *TP53* mutation.[6,7]

Targeted therapies using combined BRAF and MEK inhibition in $BRAF^{V600E}$-mutant ATC can result in a good response, but acquired resistance is common with no effective alternative treatments.[8] One reason for acquired resistance could be because both drugs act largely on the same signaling pathway; this approach is not effective when there is activation of alternate compensatory pathways.[9] One mechanism leading to acquired resistance is through persistently activating tyrosine kinase (TK) signaling by several alternative pathways.[10] Combined BRAF and MEK inhibition in $BRAF^{V600E}$-mutant ATC and other cancers is also commonly associated with treatment-related toxicity that requires a dose reduction.[11–13] To identify alternative treatments for $BRAF^{V600E}$-mutant ATC, we used drug matrix screening in $BRAF^{V600E}$ ATC cells to select highly active compounds identified from high-throughput drug screening studies, in combination with BRAF inhibition.

Combining BRAF inhibition and multitargeting tyrosine kinase inhibitors (MTKIs) had the highest synergistic/additive activity.[14] We tested ponatinib, one of the MTKIs identified to be synergistic with BRAF inhibition in $BRAF^{V600E}$-mutant ATC cells in our drug matrix screening studies. It synergistically and significantly inhibited cell proliferation, colony formation, invasion, and migration by downregulating the phospho-ERK/MEK and the c-JUN signaling pathways.[14] Axitinib is another MTKI which also showed a synergistic activity in our initial drug matrix screening with PLX4720 (a BRAF inhibitor).

Axitinib potently inhibits vascular endothelial growth factor receptor (VEGFR) and has been shown to have antitumor activity in advanced thyroid cancer.[15] It has also been reported that combination of axitinib with chemotherapeutic agents (carboplatin and paclitaxel) is well tolerated and effective in *BRAF* wild-type ($BRAF^{WT}$) metastatic melanoma.[16] VEGF is overexpressed in cancer including ATC and plays an important role in angiogenesis and immune suppression in the tumor microenvironment.[17,18] In addition, a recent study reported that VEGF was strongly expressed in malignant thyroid lesions,[19] and upregulation of VEGF in human thyroid carcinoma is associated with a poor prognosis.[17,18,20] As mentioned above axitinib is one of the MTKIs that had synergistic/additive activity with BRAF inhibition based on our drug matrix screening in $BRAF^{V600E}$-mutant ATC cells.

The effects of combining axitinib and BRAF inhibition have not been investigated in $BRAF^{V600E}$-mutant ATC. Based on these reports and our findings, we hypothesized that MTKIs in combination with BRAF inhibition may have synergistic/additive activity in $BRAF^{V600E}$-mutant ATC by targeting additional activated kinase signaling pathways, and thus investigated the novel combination of axitinib and BRAF inhibition in *in vitro* and *in vivo* models of $BRAF^{V600E}$-mutant ATC.

Materials and Methods

Cell lines and culture conditions

ATC cell lines 8505C and SW1736 harboring the $BRAF^{V600E}$ mutation were purchased from the European Collection of Cell Culture (Salisbury, United Kingdom) and Cell Lines Service GmbH (Eppelheim, Germany), respectively. The $BRAF^{WT}$ cell line THJ16T derived from a patient with ATC was kindly gifted by Dr. John A. Copland (Mayo Clinic, Jacksonville, FL) (Supplementary Method).

Cell proliferation assay

Cell proliferation assays were performed in triplicate to evaluate the effect of the drugs on cell viability using the CyQUANT kit according to manufacturer's instructions (Cat. No. C7026; Thermo Fisher Scientific, Waltham, MA) (Supplementary Method).

Clonogenic assay

Clonogenic assay with both short-term and long-term drug treatment was performed using standardized protocol (Supplementary Method).

Migration assay

A scratch plate or wound healing assay was performed to assess the effect of the drugs on cell migration (Supplementary Method).

Invasion assay

Invasion assay was performed according to the manufacturer's instructions (QCM ECMatrix Cell Invasion Assay, Cat. No. ECM550; Millipore Sigma, Burlington, MA) (Supplementary Method).

Cell cycle analysis

Cells were treated for 24–72 hours, fixed, then stained and analyzed by Flow cytometry FxCycle™ PI/RNase Staining solution (Cat. No. F10797; Thermo Fisher Scientific) (Supplementary Method).

Phosphoprotein kinase array

We used the Proteome Profiler Human-Phospho-Kinase Array Kit (Cat. No. ARY003B; R&D Systems, Minneapolis, MN) to detect changes in phosphoprotein levels in the SW1736 cell line according to the manufacturer's instructions (Supplementary Method).

Western blot analysis

Total cell lysates from all groups were prepared and resolved by electrophoresis followed by Western blot analysis using standardized method (Supplementary Method).

Orthotopic xenograft ATC models

All animal studies were performed according to the institutional animal care and use committee (IACUC) and Stanford Medicine guidelines. The animal protocol was reviewed and approved by the Administrative Panel on Laboratory Animal Care (APLAC) and the APLAC protocol number is APLAC-34003. For the orthotopic ATC model, 1×10^6 8505C-Luc2 cells (Luc2 denotes cells with stable expression of a luciferase reporter) were injected into the thyroid gland of *NOD Cg-Prkdc*^{cid} *Il2rg*^{tm1Wjl}*/SzJ* mice. Two weeks after orthotopic implantation, mice were randomized into five treatment groups ($n = 8$ per group). Each group was treated for

2 weeks, and at the end of the treatment, all mice were sacrificed using CO_2 inhalation. Tumor volumes were measured using electronic calipers. Tumor, lung, and liver tissues were collected both by snap freezing (for RNA and protein isolations) as well as in 4% paraformaldehyde (for immunohistochemistry). Please see Supplementary Method for details.

Statistical analyses

The data are presented as the mean ± standard error of the mean or mean ± standard deviation and GraphPad Prism version 8 (GraphPad Software, Inc., San Diego, CA) was used to perform all statistical analyses (Supplementary Method).

Results

Combination of BRAF inhibitors (PLX4720 and dabrafenib) and axitinib decreases cell proliferation in BRAF^{V600E}*-mutant ATC cells*

As expected, dabrafenib treatment inhibited cellular proliferation, colony formation (both short term and long term), and migration of 8505C and SW1736 ATC cell lines that was mostly dose-dependent (Supplementary Fig. S1A–E). We selected 10 μM of dabrafenib in combination with 1.89 μM axitinib for the follow-up studies as the combination had the highest inhibitory effect on cellular proliferation compared to single agents in both the cell lines (Supplementary Fig. S2A). Both dabrafenib and PLX4720 are *BRAF*^{V600E} inhibitors that can block the ERK pathway in *BRAF*^{V600E}-mutant ATC cells and both inhibitors downregulated p42/44 ERK in the 8505c and SW1736 cell lines after treatment for 24 hours. Axitinib alone did not affect the ERK pathway in 8505c and SW1736 cells at that time point.

The combination of PLX4720 or dabrafenib with axitinib also led to the downregulation of phospho-ERK in 8505C and SW1736 cells compared to control and axitinib treatment alone (Supplementary Fig. S3A, B). The inhibitory effect of axitinib on VEGFR signaling has been shown to be mediate through STAT3[21–23] and/or AKT[24–26] pathways in previous studies. Thus, we analyzed phospho-STAT3 and AKT levels with axitinib treatment to confirm its target effect and found decreased phospho-STAT3 and AKT levels with axitinib treatment in 8505C (Supplementary Fig. S3C, D).

The proliferation assay showed that the combination of PLX4720 and axitinib inhibited cell proliferation significantly more compared with single agents in all three ATC cell lines: two *BRAF*^{V600E}-mutant ATC cell lines (8505C and SW1736) and one *BRAF*^{WT} ATC cell line THJ16T ($p < 0.0001$, $p < 0.001$, and $p < 0.01$, respectively) (Fig. 1A). The combination of dabrafenib and axitinib also significantly inhibited cell proliferation compared with either compound alone in 8505C cells ($p < 0.0001$ and $p < 0.001$, respectively) and compared with dabrafenib alone in SW1736 and THJ16T cells ($p < 0.05$ and $p < 0.0001$, respectively) (Fig. 1A). We used the Chou–Talaley algorithm to check the nature of the drug combination interaction. PLX4720 or dabrafenib with axitinib had a mainly synergistic or additive effect on *BRAF*^{V600E}-mutant ATC 8505C and SW1736 cells, whereas the drug interaction was mainly antagonistic in *BRAF*^{WT} THJ16T cells (Fig. 1B, C).

Based on the cellular proliferation assays, we selected a combination dose which had the highest effect as compared to single agents (Supplementary Fig. S2A) to conduct the additional experiments using the *BRAF*^{V600E}-mutant ATC 8505C and SW1736 cell lines.

Combination of BRAF inhibitors (PLX4720 and dabrafenib) and axitinib inhibits colony formation and cell migration and invasion in BRAF^{V600E}*-mutant ATC cells*

We used PLX4720 (15 μM) and dabrafenib (10 μM) alone or in combination with two different concentrations of axitinib (1.89 and 0.47 μM). A high axitinib concentration (1.89 μM) used alone was very effective in inhibiting colony formation in both 8505C and SW1736C cells compared with a low concentration (0.47 μM). The combination of PLX4720 (15 μM) and the higher (1.89 μM) and lower (0.47 μM) axitinib concentrations was significantly more effective in inhibiting colony formation in 8505c and SW1736 cells compared with vehicle ($p < 0.0001$) and PLX4720 alone ($p < 0.0001$) (Fig. 1D, E). Similarly, the combination of dabrafenib (10 μM) and both axitinib concentrations significantly inhibited colony formation in 8505C and SW1736 cells compared with vehicle and dabrafenib alone ($p < 0.0001$ and $p < 0.0001$, respectively) (Fig. 1D, E). Both the drug combinations were significantly more effective than 0.47 μM axitinib alone and the BRAF inhibitors alone ($p < 0.0001$, $p < 0.001$, $p < 0.01$, $p < 0.05$) (Supplementary Fig. S4A, B). Long-term treatment also showed similar effects in the colony formation assay (Supplementary Fig. S4C).

Treatment with both PLX4720 (15 μM) and axitinib (1.89 μM) significantly inhibited cell migration compared with vehicle ($p < 0.0001$), PLX4720 ($p < 0.01$ and $p < 0.05$), and axitinib ($p < 0.0001$) in both *BRAF*^{V600E}-mutant ATC cell lines (Fig. 2A, B). Similarly, the combination of dabrafenib and axitinib significantly reduced cell migration compared with vehicle ($p < 0.0001$) and axitinib alone ($p < 0.0001$) in 8505C and SW1736 cells. However, compared with dabrafenib alone, the combination of dabrafenib and axitinib was effective in inhibiting cell migration in 8505C cells, while it showed less of an effect in SW1736 cells.

In both 8505C and SW1736 cells, the combination of PLX4720 and axitinib significantly inhibited cell invasion compared with vehicle ($p < 0.0001$), PLX4720 ($p < 0.01$), and axitinib ($p < 0.01$) (Fig. 2C, D). The combination of dabrafenib and axitinib significantly inhibited cell invasion compared with vehicle ($p < 0.001$) and dabrafenib ($p < 0.01$) in SW1736 cells but only compared with vehicle in 8505C cells ($p < 0.0001$).

Combination of BRAF inhibitors (PLX4720 and dabrafenib) and axitinib causes cell cycle arrest in BRAF^{V600E}*-mutant ATC cells*

Overall, the combination of BRAF inhibitors and axitinib showed additive anticancer activity in ATC cells, so we next investigated the mechanism(s) of action for this additive effect. BRAF inhibitors have been reported to arrest the cell cycle, so we evaluated how each agent alone and in combination affected the cell cycle.[27,28] When used alone, the BRAF inhibitors PLX4720 and dabrafenib arrested 8505c and SW1736 cells in the G1/G0 phase within 24 hours of treatment (Fig. 3A). Screening for the effect of these drugs on the expression and function of critical cell cycle checkpoint proteins showed that

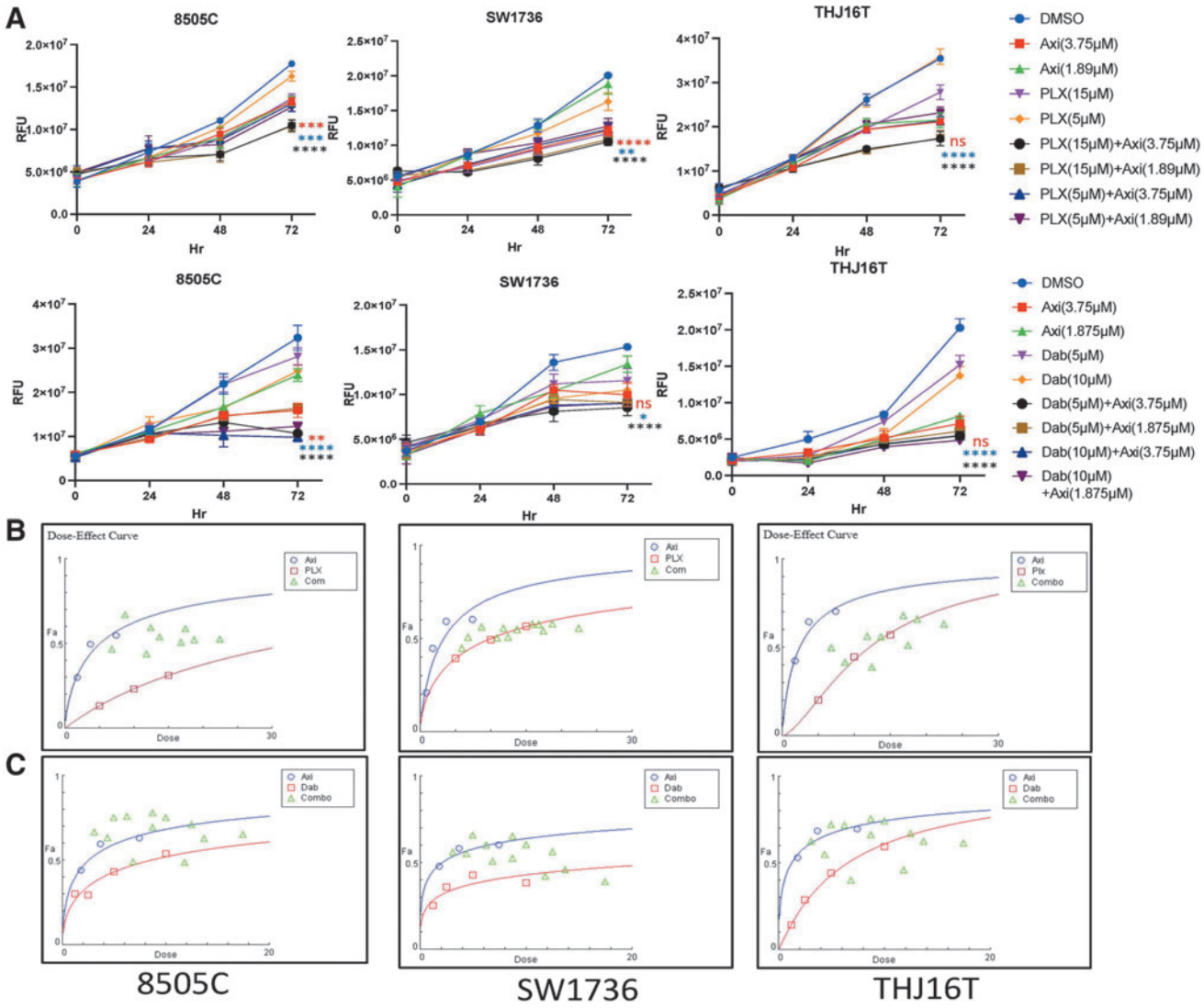

FIG. 1. Combination BRAF inhibition (PLX4720 and dabrafenib) and axitinib treatment decreases cell proliferation and colony formation in *BRAF*^{V600E}-mutant ATC cells. (**A**) The effect of axitinib, dabrafenib, and PLX4720 alone and in combination on cell proliferation. Cell viability was analyzed for treatment with PLX4720 (5 and 15 μM), dabrafenib (5 and 10 μM), axitinib (1.87 and 3.75 μM), or the combination of each BRAF inhibitor and axitinib for up to 72 hours. The *x*-axis represents the elapsed time in hours and the *y*-axis represents RFU. The combination of PLX4720 and axitinib and the combination of dabrafenib and axitinib inhibited cell proliferation significantly more in all cell lines (8505C, SW1736, and THJ16T) compared with vehicle and each BRAF inhibitor alone ($p < 0.0001$) after 72 hours of treatment. The data are presented as the mean ± SD. (**B, C**) The combination index indicating the type of association for PLX4720 and axitinib (top panel) and dabrafenib and axitinib treatment (bottom panel) in *BRAF*^{V600E}-mutant ATC cell lines is depicted as an isobologram of drug combinations. The *x*-axis represents the drug concentration, and the *y*-axis represents their combination effect at fraction affected (Fa) of 0.5 (50% reduction in cell growth). The red and blue plots are the response to single agents; the combination plots (green) indicate a mostly additive effect when cell growth inhibition was greater than ~50% (Fa = 0.50–0.90). (**D**) The combination of a BRAF inhibitor and axitinib inhibited colony formation. PLX4720 (15 μM) and axitinib (1.89 and 0.47 μM) reduced colony formation significantly more than vehicle and PLX4720 alone in 8505C and SW1736 cells ($p < 0.0001$). Dabrafenib (10 μM) and axitinib (1.89 and 0.47 μM) also reduced colony formation significantly more compared with vehicle ($p < 0.0001$) and dabrafenib alone ($p < 0.01$). (**E**) The histogram represents the mean colony counts of 8505C and SW1736 cells. The data are shown as the mean ± SD. For all panels, the black stars denote combination versus vehicle, the blue stars denote combination versus BRAF inhibitor (PLX4720 and dabrafenib), and the red stars denote combination versus axitinib. ATC, anaplastic thyroid cancer; Axi, axitinib; Dab, dabrafenib; PLX, PLX4720; RFU, relative fluorescence units; SD, standard deviation.

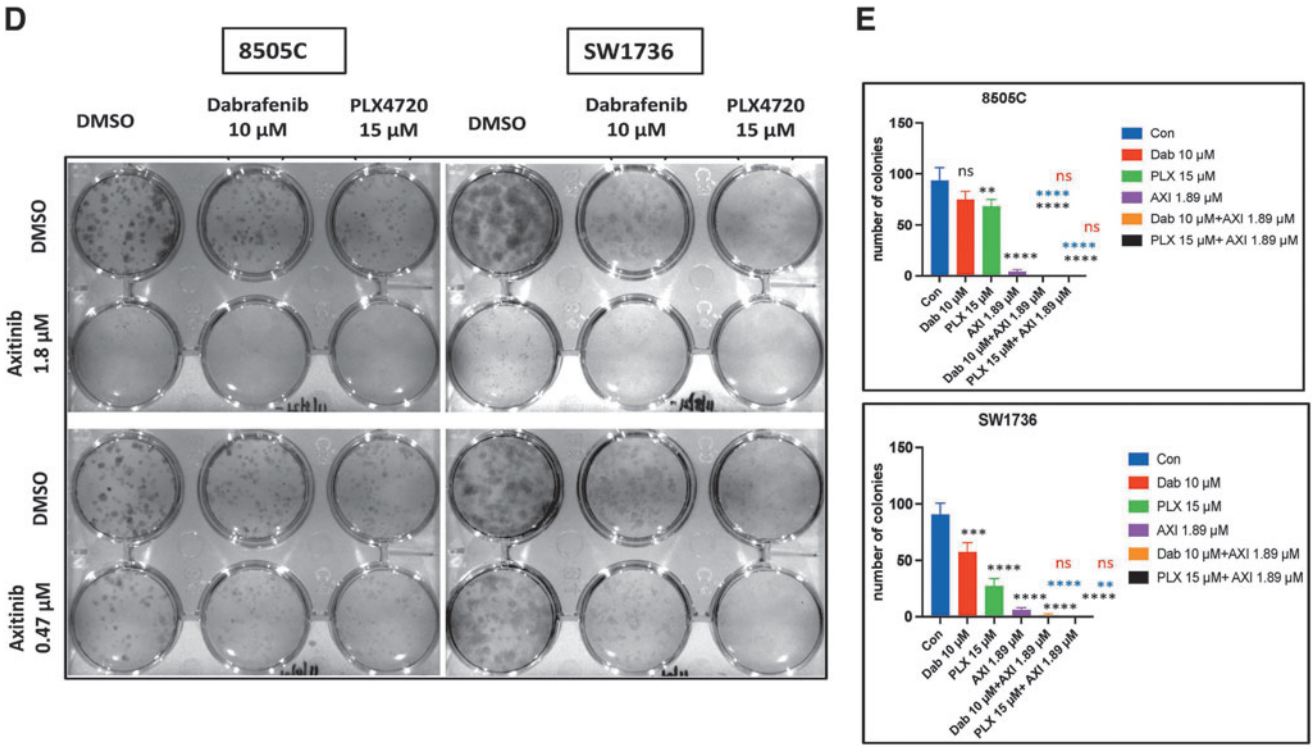

FIG. 1. (*Continued*).

treatment with PLX4720 and dabrafenib alone and in combination with axitinib significantly reduced the expression of cyclin A2, cyclin D1, and cyclin E2 while increasing the expression of p21 Waf1 and p27 kip in 8505C and SW1736 cells (Fig. 3B). Moreover, treatment with axitinib alone resulted in a significant number of 8505c and SW1736 cells arrested in the G2/M phase of the cell cycle (Fig. 3A). Axitinib increased cyclin B1 expression but had no effect on the expression of the other cell cycle checkpoint proteins studied (Fig. 3B).

Combined fluorescence-activated cell sorting (FACS) and Western blot analysis of the cell cycle regulatory proteins in 8505c and SW1736 cells treated with axitinib and BRAF inhibitors suggested that the cells are arrested in either the G0/G1 or G2/M phase (Fig. 3C).

Axitinib decreases phosphorylation of aurora kinase B and histone H3A levels in BRAF^{V600E}*-mutant ATC cells*

Although axitinib did not affect most of the analyzed cell cycle checkpoint proteins, it arrested the cells in the G2/M phase. This finding led us to investigate the effect of axitinib on other critical steps involved in mitosis. Thus, we examined the role of axitinib on regulatory proteins that have a role in chromosomal organization. One of the proteins of interest is aurora kinase B (AURKB), which gets phosphorylated during the cell cycle and is involved in chromosomal organization.[29] Treatment with axitinib alone and in combination with PLX4720 or dabrafenib decreased phosphorylation of AURKB Thr232 and histone 3A (H3A) Ser10 in the ATC cell lines (Fig. 4A). These results suggest that axitinib's inhibition of AURKB phosphorylation decreases the phosphorylation of H3A Ser10, resulting in blockade of the metaphase-to-anaphase transition. This causes the cells to accumulate in the G2/M phase during the cell cycle (Fig. 4B).

Axitinib increases c-JUN levels in BRAF^{V600E}*-mutant ATC cells*

To understand the regulatory signaling pathways that are affected with axitinib treatment in *BRAF*^{V600E}-mutant ATC cells, we used the Proteome Profiler Human-Phospho-Kinase

FIG. 2. The combination of BRAF inhibition and axitinib treatment inhibits cell migration and invasion in *BRAF*^{V600E}-mutant ATC cells. (**A**) The combination of PLX4720 (15 μM) and axitinib (1.89 μM) significantly inhibited cell migration compared with vehicle ($p<0.0001$), PLX4720 ($p<0.01$ and $p<0.05$), and axitinib ($p<0.0001$) in both cell lines. The combination of dabrafenib and axitinib significantly reduced cell migration compared with vehicle ($p<0.0001$) and axitinib ($p<0.0001$) in both cell lines 24 hours after scratching. (**B**) The histogram represents the mean wound area remaining 24 hours after scratching 8505C and SW1736 cells. The data are shown as the mean ± SD. (**C**) PLX4720 and axitinib treatment significantly reduced cell invasion after 24 hours compared with vehicle ($p<0.0001$ and $p<0.001$), PLX4720 ($p<0.001$), and axitinib ($p<0.001$) in 8505C and SW1736 cells. The combination of dabrafenib and axitinib inhibited cell invasion significantly more compared with vehicle ($p<0.0001$ and $p<0.001$) in both cell lines. (**D**) The histogram represents the mean number of cells that invaded the membrane/field of image. The data are shown as the mean ± SD. For all panels, the black stars denote combination versus vehicle, the blue stars denote combination versus BRAF inhibitor (PLX4720 and dabrafenib), and the red stars denote combination versus axitinib.

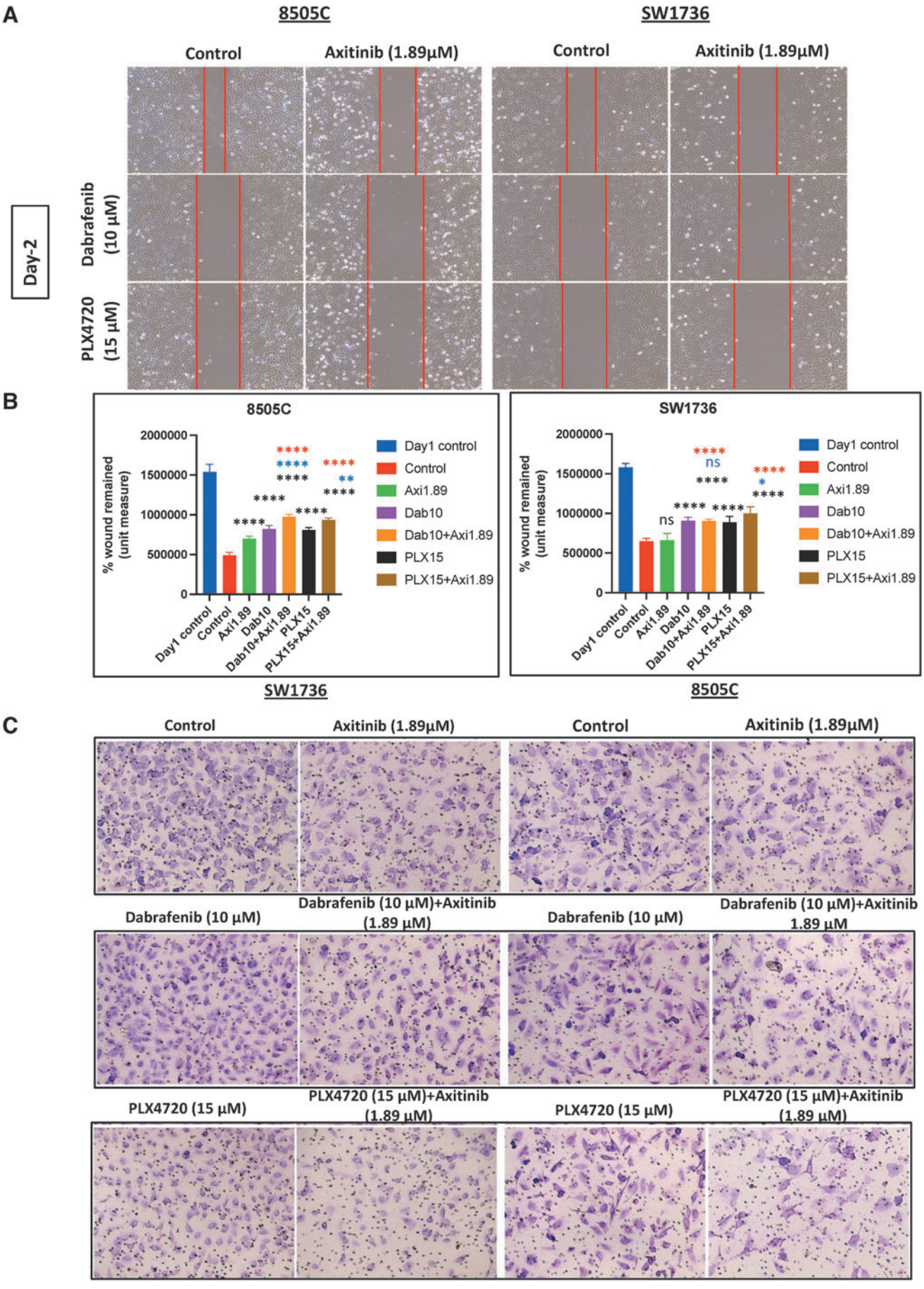
A
8505C
SW1736
Control
Axitinib (1.89μM)
Control
Axitinib (1.89μM)
Day-2
Dabrafenib (10 μM)
PLX4720 (15 μM)
B
8505C
SW1736
% wound remained (unit measure)
2000000
1500000
1000000
500000
0
Day1 control
Control
Axi1.89
Dab10
Dab10+Axi1.89
PLX15
PLX15+Axi1.89
****
**
*
ns
SW1736
8505C
C
Control
Axitinib (1.89μM)
Control
Axitinib (1.89μM)
Dabrafenib (10 μM)
Dabrafenib (10 μM)+Axitinib (1.89 μM)
Dabrafenib (10 μM)
Dabrafenib (10 μM)+Axitinib 1.89 μM
PLX4720 (15 μM)
PLX4720 (15 μM)+Axitinib (1.89 μM)
PLX4720 (15 μM)
PLX4720 (15 μM)+Axitinib (1.89 μM)

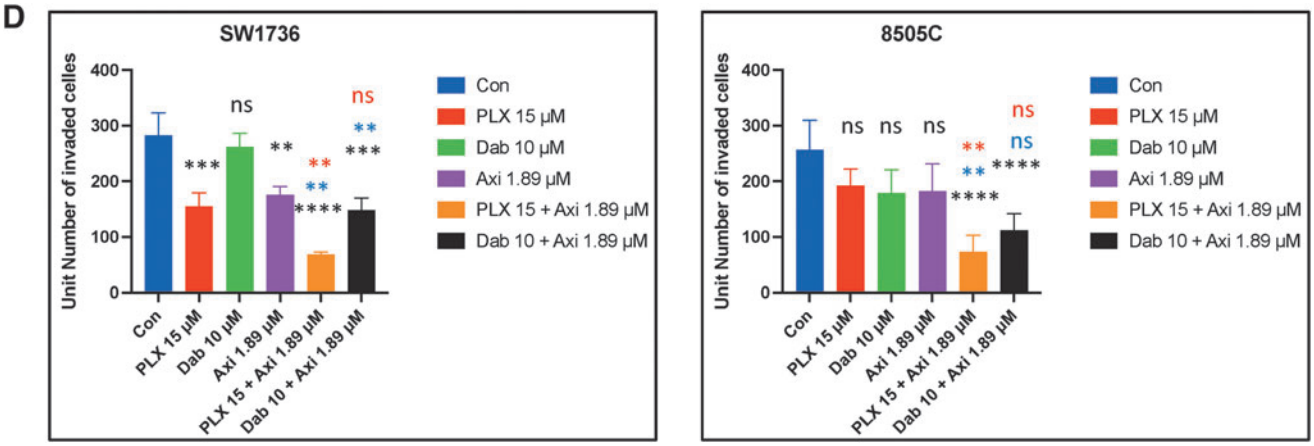

FIG. 2. (*Continued*).

Array. As expected, treatment with the BRAF inhibitor dabrafenib alone and in combination with axitinib reduced ERK phosphorylation, confirming the accuracy of the assay (Fig. 4C). Axitinib increased the phosphorylation of c-JUN (Ser63) in SW1736 cells (Fig. 4C). We validated the increase in c-JUN phosphorylation after axitinib treatment by Western blot analysis (Fig. 4D). c-JUN phosphorylation plays a role in G2/M arrest by increasing cyclin B1.[30,31] This suggests that the effect of axitinib treatment in inducing G2/M cell cycle arrest is also due to its effect on c-JUN phosphorylation.

Combination of BRAF inhibitors and axitinib reduces tumor growth in vivo

We orthotopically implanted 8505c-Luc2 cells into the thyroid gland of *NOD Cg-Prkdcs*^{cid} *Il2rg*^{tm1Wjl}*/SzJ* mice. Two weeks after implanting 1×10^6 cells, when the tumor volume was $\sim$50–60 mm^3, we randomized the mice to the following treatment groups: vehicle; axitinib, PLX4720, or dabrafenib alone; or the combination of axitinib with PLX4720 or dabrafenib. Four weeks after implantation, we sacrificed the mice and compared their tumor volumes.

Mice in the axitinib, PLX4720, and dabrafenib groups showed significantly decreased tumor volumes compared with mice in the vehicle group ($p < 0.0001$). The combination treatments were even more effective in reducing tumor volumes than the single treatments (Fig. 5A–C). Mice receiving combination treatment showed a significant reduction in the tumor volume compared with mice in the vehicle group: PLX4720+axitinib (15.43 ± 6.6 mm^3 vs. 96.92 ± 20.8 mm^3, $p < 0.0001$) and dabrafenib+axitinib (12.63 ± 4.5 mm^3 vs. 96.92 ± 20.8 mm^3, $p < 0.0001$) (Fig. 5A–C; Supplementary Fig. S5). Mice in the vehicle group (13 ± 1 g), the PLX4720 group (15.625 ± 1.5 g), the dabrafenib group (16.5 ± 2.1 g), and the axitinib group (14.75 ± 2.52 g) had much lower body weights than mice in the PLX4720+axitinib group (18 ± 2 g) and the dabrafenib+axitinib group (17.75 ± 1.98 g), who not only maintained better body weight but also showed no signs of illness or decreased mobility (Fig. 5D).

Discussion

BRAF^{V600E} is one of the most common driver mutations found in ATC and has been effectively targeted in patients with ATC by using BRAF and MEK inhibitors.[32] Unfortunately, most patients with ATC and *BRAF*^{V600E} mutation develop resistance to targeted therapy with BRAF and MEK inhibitors.[33,34] Although the exact mechanisms of resistance toward BRAF inhibitors are still under investigation, researchers have reported feedback activation of the RAS pathway and rewiring of the entire MAPK pathway upon long-term use of BRAF inhibitors.[34] Combination treatment with the BRAF inhibitor dabrafenib and the MEK inhibitor trametinib is a clinically approved treatment in *BRAF*^{V600E}-mutant ATC as well as melanoma and squamous cell carcinoma of the lung.[12,35] However, studies have shown a novel mechanism of developing resistance toward BRAF and MEK inhibitors after a good response rate in different types of cancers because both of

FIG. 3. Effect of combination BRAF inhibition and axitinib treatment on cell cycle in *BRAF*^{V600E}-mutant ATC cells. (**A**) The combination of BRAF inhibition and axitinib causes cell cycle arrest. The BRAF inhibitors PLX4720 and dabrafenib caused G1/G0 arrest in 8505C and SW1736 cells 24 hours after treatment. Axitinib caused G2/M arrest after 24 hours in both cell lines. The combination of PLX4720 and axitinib and the combination of dabrafenib and axitinib caused either G1/G0 or G2/M arrest in 8505C and SW1736 cells, thus inhibiting their proliferation. The *x*-axis indicates the cell count, and the *y*-axis indicates propidium iodide staining. (**B**) Western blot of the cell cycle checkpoint proteins cyclin B1, cyclin A2, cyclin D1, cyclin E2, p21, and p27 kip in 8505C and SW1736 cells after treatment for 24 hours with BRAF inhibitors (PLX4720, dabrafenib) and axitinib alone and in combination. (**C**) Graphical representation of the mechanism of a BRAF inhibitor on the cell cycle as identified from FACS and Western blot analysis. The BRAF inhibitors PLX4720 and dabrafenib increase the expression of p21 and p27, causing G1/G0 cell cycle arrest. FACS, fluorescence activated cell sorting.

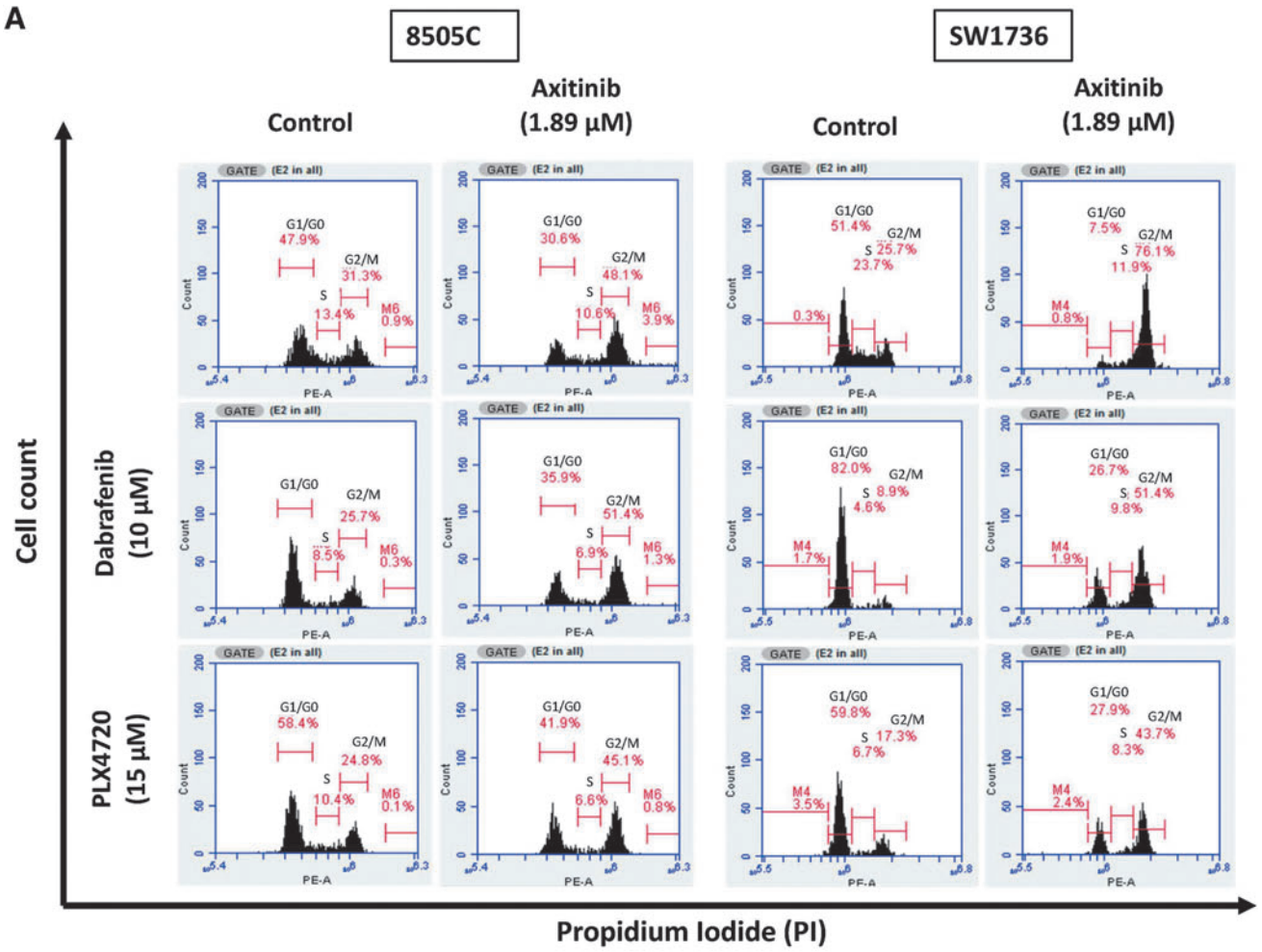
A
8505C
SW1736
Control
Axitinib (1.89 μM)
Control
Axitinib (1.89 μM)
Cell count
Dabrafenib (10 μM)
PLX4720 (15 μM)
Propidium Iodide (PI)
GATE (E2 in all)
PE-A
Count
G1/G0 47.9%
G2/M 31.3%
S 13.4%
M6 0.9%
G1/G0 30.6%
G2/M 48.1%
S 10.6%
M6 3.9%
G1/G0 51.4%
G2/M 25.7%
S 23.7%
0.3%
G1/G0 7.5%
G2/M 76.1%
S 11.9%
M4 0.8%
G1/G0 58.4%
G2/M 24.8%
S 10.4%
M6 0.1%
G1/G0 41.9%
G2/M 45.1%
S 6.6%
M6 0.8%
G1/G0 59.8%
G2/M 17.3%
S 6.7%
M4 3.5%
G1/G0 27.9%
G2/M 43.7%
S 8.3%
M4 2.4%
G1/G0 35.9%
G2/M 51.4%
S 6.9%
M6 1.3%
G1/G0 82.0%
G2/M 8.9%
S 4.6%
M4 1.7%
G1/G0 26.7%
G2/M 51.4%
S 9.8%
M4 1.9%
G1/G0 47.9%
G2/M 25.7%
S 8.5%
M6 0.3%

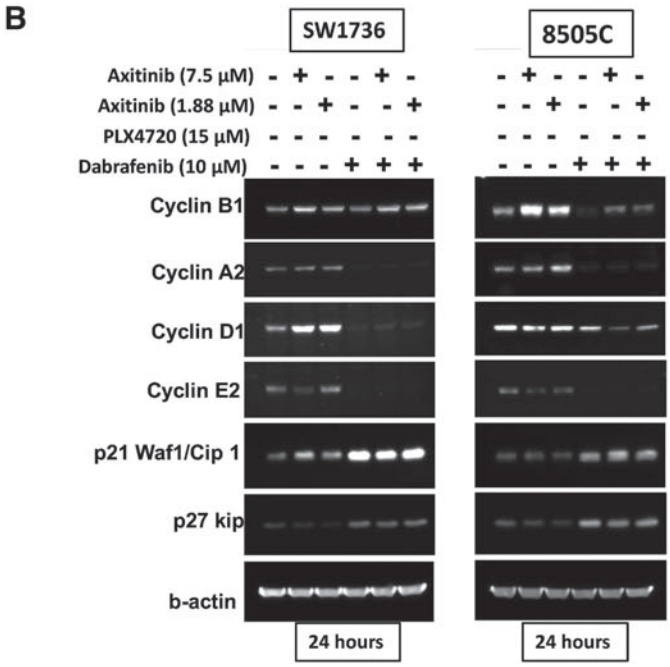
B
SW1736
8505C
Axitinib (7.5 μM)
Axitinib (1.88 μM)
PLX4720 (15 μM)
Dabrafenib (10 μM)
Cyclin B1
Cyclin A2
Cyclin D1
Cyclin E2
p21 Waf1/Cip 1
p27 kip
b-actin
24 hours
24 hours

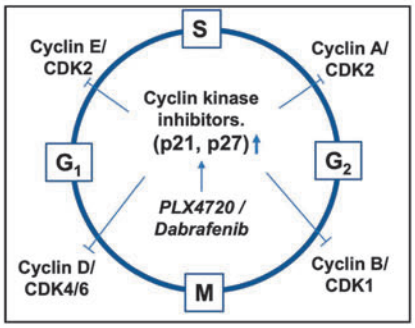
C
S
Cyclin E/ CDK2
Cyclin A/ CDK2
Cyclin kinase inhibitors. (p21, p27)
G1
G2
PLX4720 / Dabrafenib
Cyclin D/ CDK4/6
Cyclin B/ CDK1
M

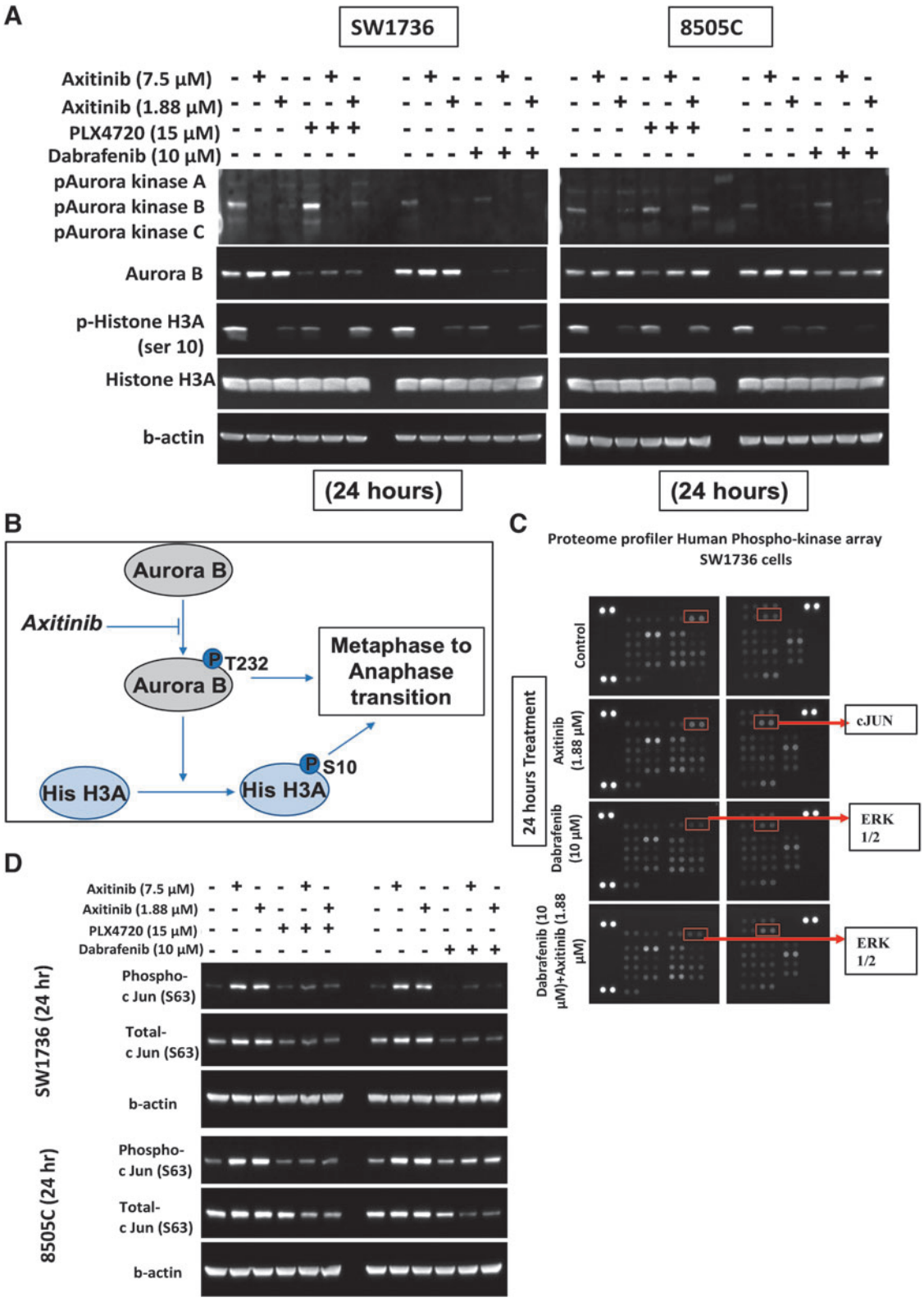

FIG. 4. Mechanism of action of axitinib treatment and in combination with BRAF inhibition in *BRAF*^{V600E}-mutant ATC cells. (**A**) Western blot analysis showing that axitinib inhibited the expression of phosphorylated aurora kinase B and phosphorylated histone H3A in 8505C and SW1736 cells after 24 hours of treatment. (**B**) Graphical representation of the mechanism of action of axitinib. It inhibits phosphorylation of aurora kinase B, which inhibits the phosphorylation of histone 3A, a protein that is required for the metaphase-to-anaphase transition. The overall effect is G2/M cell cycle arrest. (**C**) The Proteome Profiler Human-Phospho-Kinase Array for SW1736 cells using one BRAF inhibitor (dabrafenib) and axitinib treatment alone and in combination for 24 hours showed increased phospho-c-JUN after axitinib and combination treatment. (**D**) Western blot analysis to validate the Proteome Profiler Human-Phospho-Kinase Array data for both cell lines using both BRAF inhibitors. Axitinib reduced the expression of phospho-c-JUN and total c-JUN in 8505C and SW1736 cells after treatment for 24 hours. H3A, histone 3A.

these drugs target the MAPK pathway, and thus various feedback mechanisms are activated.[36–40]

Thus, preclinical studies exploring other novel combination treatments that target different pathways are needed in *BRAF*^{V600E}-mutant ATC and could lower the rate of treatment resistance.[41–43] We previously performed a drug matrix screening of compounds with high anticancer activity in combination with BRAF inhibition in *BRAF*^{V600E}-mutant ATC cells; MTKIs had some of the highest synergistic and additive activity.[14] In this study, we have reported for the first time that the combination of a BRAF inhibitor (PLX4720 and dabrafenib) and axitinib has additive anticancer activity in *BRAF*^{V600E}-mutant ATC based on *in vitro* and *in vivo* studies.

Axitinib is in clinical use with other agents (e.g., avelumab, pembrolizumab) as a first-line treatment for advanced renal cell carcinoma (RCC),[44,45] or as a second-line treatment for RCC.[46,47] Axitinib is also being evaluated in clinical trials in other cancers such as head and neck cancers,[48] and advance stage thyroid cancer.[49] These clinical trials showed axitinib has anti-cancer activity and is associated with improved overall survival as well as having an acceptable safety profile with manageable side effects. Lenvatinib is a currently approved MTKI for differentiated thyroid cancer that fails standard therapy but has a high rate of serious treatment-related adverse effects and is not effective in ATC.[50] Thus, alternative MTKI treatment options are needed.

In our initial drug matrix screening, we identified that PLX4720 and axitinib have higher combination activity (based on the mean highest single agent model [HSA] and mean bliss independence model [BLISS] scores) as compared to vemurafenib and axitinib. PLX4720 also has increased inhibition of BRAF at a lower concentration in cell-free assays compared to vemurafenib. Vemurafenib treatment can result in resistance.[51–54] Thus, in this study, we evaluated PLX4720 and dabrafenib as the BRAF inhibitors in combination with axitinib.

Both the combinations showed more effective inhibition of cell growth by inducing cell cycle arrest mediated through known regulators of the cell cycle; decreased expression of cyclins; and decreased phosphorylation of AURKB (Thr232) and histone H3 (Ser10). Both BRAF inhibitors induced G1/G0 arrest and axitinib induced G2/M arrest, which is consistent with previous studies.[27,28,55] Interestingly, we observed G2/M arrest when we used BRAF inhibitors alongside axitinib. Our data suggest that BRAF inhibitors alone and in combination with axitinib induce the cyclin inhibitors p21 Waf1 and p27 kip, changes that ultimately inhibit the checkpoint cyclins resulting in cell cycle arrest and senescence. However, axitinib treatment alone increased cyclin B1 expression, mainly at higher dose, and had no effect on the other analyzed proteins. We observed increased expression of phospho-c-JUN in ATC cells treated with axitinib. c-JUN phosphorylation has been reported to play a role in G2/M arrest by increasing cyclin B1.[31]

AURKB is another important cell cycle regulator that plays an essential role in cancer cell proliferation and has been targeted to reduce cancer cell survival by induction of G2/M arrest and apoptosis. c-JUN is an upstream regulator of the AURKB pathway.[29,56] Axitinib in combination with BRAF inhibitors also showed minimal to no significant reactivation of pERK, indicating this combination attenuates the rebound effect of pERK inhibition which is also reflected by the higher cell death observed in the combination treatment groups.[57–59]

In the current study, treatment with axitinib alone significantly inhibited tumor growth *in vivo*. However, the combination of BRAF inhibitors and axitinib inhibited tumor growth the most and improved the weight and overall health of mice, confirming its enhanced anticancer activity in *BRAF*^{V600E}-mutant ATC. Previous studies have shown that *BRAF*^{V600E}-mutant tumors treated with PLX4720 show a good initial response but it's only for limited duration as most of the patients develop resistance. In this study, we showed similar results as PLX4720-treated mice showed a good response after 2 weeks of treatment regarding tumor volume reduction, but the health of the mice started to deteriorate and they reached a humane endpoint for euthanasia before the end of our survival study. However, mice treated with both PLX4720 and axitinib showed significant improvement in survival compared with treatment with either drug alone, demonstrating that the combination of PLX4720 and axitinib can result in more durable responses and less toxicity.

In summary, combination of BRAF inhibition (PLX4720 and dabrafenib) and axitinib has enhanced anticancer activity in *BRAF*^{V600E}-mutant ATC *in vitro* and *in vivo*. This enhanced additive effect is mediated by inducing G1/G0 and G2/M cell cycle arrest. Hence, the combination of BRAF inhibitors and axitinib represents a promising new targeted therapy for *BRAF*^{V600E}-mutant ATC. Our preclinical results suggest that this combination should be tested in clinical trials.

FIG. 5. Effect of combination BRAF inhibition and axitinib treatment *in vivo*. (**A, B**) The combination of BRAF inhibitors and axitinib reduces tumor growth *in vivo*. The combination of PLX4720 and axitinib significantly reduced tumor growth compared with vehicle group (84%, $p < 0.0001$) and the PLX4720 group ($p < 0.01$). In the groups treated with each agent alone (PLX4720, 62%; axitinib, 70%), there was significant difference compared with the vehicle group ($p < 0.0001$). The combination of dabrafenib and axitinib significantly reduced tumor growth compared with the vehicle group (86%, $p < 0.0001$) and the dabrafenib group ($p < 0.01$). In the dabrafenib group (Dab, 61%), there was a significant difference compared with the vehicle group ($p < 0.0001$). (**C**) Pathological representative images of H and E staining of thyroid tumor from each group (original × 4 size). (**D**) The mice in the dabrafenib, PLX720+axitinib, and dabrafenib+axitinib groups weighed significantly more than the mice in the vehicle group ($p < 0.0001$) and the axitinib group ($p < 0.01$) on the last day of treatment (day 14). The mice in the vehicle, PLX4720, and axitinib groups had significantly lower body weights compared with the combination treatment group (29.4 ± 3.2 g; $p < 0.05$), who maintained their body weight and showed no signs of illness or cachexia. For all panels, the black stars denote vehicle versus other groups, the blue stars denote BRAF inhibitor (PLX4720 and dabrafenib) vs combination groups, and the red stars denote axitinib vs combination groups.

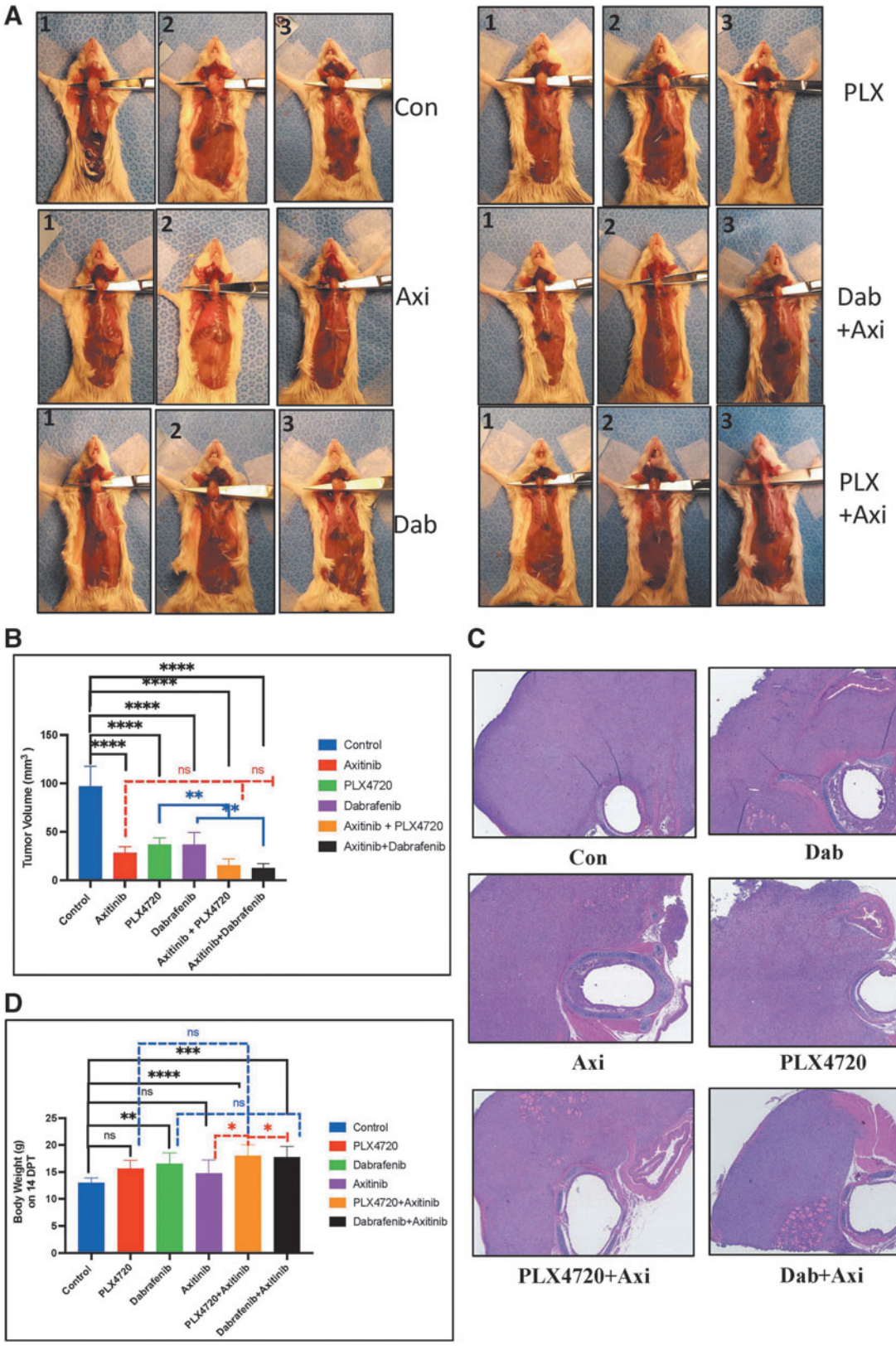
A
Con
Axi
Dab
PLX
Dab
+Axi
PLX
+Axi
B
Tumor Volume (mm3)
Control
Axitinib
PLX4720
Dabrafenib
Axitinib + PLX4720
Axitinib+Dabrafenib
C
Con
Dab
Axi
PLX4720
PLX4720+Axi
Dab+Axi
D
Body Weight (g) on 14 DPT
Control
PLX4720
Dabrafenib
Axitinib
PLX4720+Axitinib
Dabrafenib+Axitinib

Acknowledgment

Part of the data reported in this study was presented at the 2021 American Thyroid Association annual meeting (Abstract ID poster-66).

Authors' Contributions

Conception and design: V.G., C.G., E.K. Development of methodology: V.G., C.G., E.K. Acquisition of data (provided animals, acquired, and managed patients, provided facilities, etc.): E.K., C.G., V.G., J.H., L.Z., M.S., Y.Z. Analysis and interpretation of data (e.g., statistical analysis, biostatistics, computational analysis): C.G., V.G., J.H., L.Z., M.S., Y.Z., E.K. Writing, review of the manuscript: C.G., V.G., J.H., E.K., L.Z., M.S., Y.Z. Administrative, technical, or material support (i.e., reporting or organizing data, constructing databases): C.G., V.G., E.K. Study supervision: E.K. Other (acquisition of experimental data): C.G., V.G., J.H. L.Z., M.S., Y.Z., E.K. All authors reviewed and approved the final version of the article.

Author Disclosure Statement

All authors declare that they have no competing financial interest.

Funding Information

Early drug screening work was supported through the National Cancer Institute, National Institutes of Health (ZIABC011286-09), and the remainder of the research was supported through the Stanford University, Stanford Medicine Harry A. Oberhelman Jr., and Mark L. Welton Endowment.

Supplementary Material

Supplementary Method
Supplementary Figure S1
Supplementary Figure S2
Supplementary Figure S3
Supplementary Figure S4
Supplementary Figure S5

References

1. Nagaiah G, Hossain A, Mooney CJ, et al. Anaplastic thyroid cancer: A review of epidemiology, pathogenesis, and treatment. J Oncol 2011;2011:542358; doi: 10.1155/2011/542358
2. Landa I, Ibrahimpasic T, Boucai L, et al. Genomic and transcriptomic hallmarks of poorly differentiated and anaplastic thyroid cancers. J Clin Invest 2016;126(3):1052–1066; doi: 10.1172/JCI85271
3. Ito K, Hanamura T, Murayama K, et al. Multimodality therapeutic outcomes in anaplastic thyroid carcinoma: Improved survival in subgroups of patients with localized primary tumors. Head Neck 2012;34(2):230–237; doi: 10.1002/hed.21721
4. Xu B, Fuchs T, Dogan S, et al. Dissecting anaplastic thyroid carcinoma: A comprehensive clinical, histologic, immunophenotypic, and molecular study of 360 cases. Thyroid 2020;30(10):1505–1517; doi: 10.1089/thy.2020.0086
5. Wang JR, Montierth M, Xu L, et al. Impact of somatic mutations on survival outcomes in patients with anaplastic thyroid carcinoma. JCO Precis Oncol 2022;6:e2100504; doi: 10.1200/PO.21.00504
6. Kunstman JW, Juhlin CC, Goh G, et al. Characterization of the mutational landscape of anaplastic thyroid cancer via whole-exome sequencing. Hum Mol Genet 2015;24(8):2318–2329; doi: 10.1093/hmg/ddu749
7. Lim AM, Taylor GR, Fellowes A, et al. BRAF inhibition in $BRAF^{V600E}$-positive anaplastic thyroid carcinoma. J Natl Compr Canc Netw 2016;14(3):249–254; doi: 10.6004/jnccn.2016.0030
8. Sanchez JN, Wang T, Cohen MS. BRAF and MEK inhibitors: Use and resistance in BRAF-mutated cancers. Drugs 2018;78(5):549–566; doi: 10.1007/s40265-018-0884-8
9. Long GV, Stroyakovskiy D, Gogas H, et al. Combined BRAF and MEK inhibition versus BRAF inhibition alone in melanoma. N Engl J Med 2014;371(20):1877–1888; doi: 10.1056/NEJMoa1406037
10. Arozarena I, Wellbrock C. Overcoming resistance to BRAF inhibitors. Ann Transl Med 2017;5(19):387; doi: 10.21037/atm.2017.06.09
11. Homan M, Warrier G, Lao CD, et al. Treatment related toxicities with combination BRAF and MEK inhibitor therapy in resected stage III melanoma. Front Oncol 2022;12:855794; doi: 10.3389/fonc.2022.855794
12. Subbiah V, Kreitman RJ, Wainberg ZA, et al. Dabrafenib plus trametinib in patients with BRAF V600E-mutant anaplastic thyroid cancer: Updated analysis from the phase II ROAR basket study. Ann Oncol 2022;33(4):406–415; doi: 10.1016/j.annonc.2021.12.014
13. Welsh SJ, Corrie PG. Management of BRAF and MEK inhibitor toxicities in patients with metastatic melanoma. Ther Adv Med Oncol 2015;7(2):122–136; doi: 10.1177/1758834014566428
14. Ghosh C, Kumar S, Kushchayeva Y, et al. A combinatorial strategy for targeting BRAF (V600E)-mutant cancers with BRAF(V600E) inhibitor (PLX4720) and tyrosine kinase inhibitor (ponatinib). Clin Cancer Res 2020;26(8):2022–2036; doi: 10.1158/1078-0432.CCR-19-1606
15. Cohen EE, Rosen LS, Vokes EE, et al. Axitinib is an active treatment for all histologic subtypes of advanced thyroid cancer: Results from a phase II study. J Clin Oncol 2008;26(29):4708–4713; doi: 10.1200/JCO.2007.15.9566
16. Algazi AP, Cha E, Ortiz-Urda SM, et al. The combination of axitinib followed by paclitaxel/carboplatin yields extended survival in advanced BRAF wild-type melanoma: Results of a clinical/correlative prospective phase II clinical trial. Br J Cancer 2015;112(8):1326–1331; doi: 10.1038/bjc.2014.541
17. Melaccio A, Sgaramella LI, Pasculli A, et al. Prognostic and therapeutic role of angiogenic microenvironment in thyroid cancer. Cancers (Basel) 2021;13(11):2775; doi: 10.3390/cancers13112775
18. Fenton C, Patel A, Dinauer C, et al. The expression of vascular endothelial growth factor and the type 1 vascular endothelial growth factor receptor correlate with the size of papillary thyroid carcinoma in children and young adults. Thyroid 2000;10(4):349–357; doi: 10.1089/thy.2000.10.349
19. Bariya D, Mishra SP, Akshay BR, et al. Relationship between vascular endothelial growth factor expression and thyroid stimulating hormone level in benign and malignant thyroid lesions. J Family Med Prim Care 2022;11(6):2565–2572; doi: 10.4103/jfmpc.jfmpc_1126_21
20. Klein M, Vignaud JM, Hennequin V, et al. Increased expression of the vascular endothelial growth factor is a pe-

jorative prognosis marker in papillary thyroid carcinoma. J Clin Endocrinol Metab 2001;86(2):656–658; doi: 10.1210/jcem.86.2.7226
21. Chen SH, Murphy DA, Lassoued W, et al. Activated STAT3 is a mediator and biomarker of VEGF endothelial activation. Cancer Biol Ther 2008;7(12):1994–2003; doi: 10.4161/cbt.7.12.6967
22. Miyazaki A, Miyake H, Fujisawa M. Molecular mechanism mediating cytotoxic activity of axitinib in sunitinib-resistant human renal cell carcinoma cells. Clin Transl Oncol 2016; 18(9):893–900; doi: 10.1007/s12094-015-1457-x
23. Dong Y, Lu B, Zhang X, et al. Cucurbitacin E, a tetracyclic triterpenes compound from Chinese medicine, inhibits tumor angiogenesis through VEGFR2-mediated Jak2-STAT3 signaling pathway. Carcinogenesis 2010;31(12):2097–2104; doi: 10.1093/carcin/bgq167
24. Hu-Lowe DD, Zou HY, Grazzini ML, et al. Nonclinical antiangiogenesis and antitumor activities of axitinib (AG-013736), an oral, potent, and selective inhibitor of vascular endothelial growth factor receptor tyrosine kinases 1, 2, 3. Clin Cancer Res 2008;14(22):7272–7283; doi: 10.1158/1078-0432.CCR-08-0652
25. Trinh XB, Tjalma WA, Vermeulen PB, et al. The VEGF pathway and the AKT/mTOR/p70S6K1 signalling pathway in human epithelial ovarian cancer. Br J Cancer 2009; 100(6):971–978; doi: 10.1038/sj.bjc.6604921
26. Kim GD, Cheong OJ, Bae SY, et al. 6″-Debromohamacanthin A, a bis (indole) alkaloid, inhibits angiogenesis by targeting the VEGFR2-mediated PI3K/AKT/mTOR signaling pathways. Mar Drugs 2013;11(4):1087–1103; doi: 10.3390/md11041087
27. Toress-Collado AX, Nazarian R, Jazirehi AR. Rescue of cell cycle progression in BRAF(V600E) inhibitor-resistant human melanoma by a chromatin modifier. Tumour Biol 2017; 39(9):1010428317721620; doi: 10.1177/1010428317721620
28. Kurata K, Onoda N, Noda S, et al. Growth arrest by activated BRAF and MEK inhibition in human anaplastic thyroid cancer cells. Int J Oncol 2016;49(6):2303–2308; doi: 10.3892/ijo.2016.3723
29. Borah NA, Sradhanjali S, Barik MR, et al. Aurora kinase B expression, its regulation and therapeutic targeting in human retinoblastoma. Invest Ophthalmol Vis Sci 2021; 62(3):16; doi: 10.1167/iovs.62.3.16
30. Prasad Tharanga Jayasooriya RG, Dilshara MG, Neelaka Molagoda IM, et al. Camptothecin induces G(2)/M phase arrest through the ATM-Chk2-Cdc25C axis as a result of autophagy-induced cytoprotection: Implications of reactive oxygen species. Oncotarget 2018;9(31):21744–21757; doi: 10.18632/oncotarget.24934
31. Yang SH, Chien CM, Chang LS, et al. Involvement of c-jun N-terminal kinase in G2/M arrest and caspase-mediated apoptosis induced by cardiotoxin III (*Naja naja atra*) in K562 leukemia cells. Toxicon 2007;49(7):966–974; doi: 10.1016/j.toxicon.2007.01.005
32. Begum S, Rosenbaum E, Henrique R, et al. BRAF mutations in anaplastic thyroid carcinoma: Implications for tumor origin, diagnosis and treatment. Mod Pathol 2004; 17(11):1359–1363; doi: 10.1038/modpathol.3800198
33. Marten KA, Gudena VK. Use of vemurafenib in anaplastic thyroid carcinoma: A case report. Cancer Biol Ther 2015;16(10):1430–1433; doi: 10.1080/15384047.2015.1071734
34. Turajlic S, Furney SJ, Stamp G, et al. Whole-genome sequencing reveals complex mechanisms of intrinsic resistance to BRAF inhibition. Ann Oncol 2014;25(5):959–967; doi: 10.1093/annonc/mdu049
35. Subbiah V, Kreitman RJ, Wainberg ZA, et al. Dabrafenib and trametinib treatment in patients with locally advanced or metastatic BRAF V600-mutant anaplastic thyroid cancer. J Clin Oncol 2018;36(1):7–13; doi: 10.1200/JCO.2017.73.6785
36. Facchinetti F, Lacroix L, Mezquita L, et al. Molecular mechanisms of resistance to BRAF and MEK inhibitors in BRAF(V600E) non-small cell lung cancer. Eur J Cancer 2020;132:211–223; doi: 10.1016/j.ejca.2020.03.025
37. Wagle N, Van Allen EM, Treacy DJ, et al. MAP kinase pathway alterations in BRAF-mutant melanoma patients with acquired resistance to combined RAF/MEK inhibition. Cancer Discov 2014;4(1):61–68; doi: 10.1158/2159-8290.CD-13-0631
38. Welsh SJ, Rizos H, Scolyer RA, et al. Resistance to combination BRAF and MEK inhibition in metastatic melanoma: Where to next? Eur J Cancer 2016;62:76–85; doi: 10.1016/j.ejca.2016.04.005
39. Johnson DB, Childress MA, Chalmers ZR, et al. BRAF internal deletions and resistance to BRAF/MEK inhibitor therapy. Pigment Cell Melanoma Res 2018;31(3):432–436; doi: 10.1111/pcmr.12674
40. Moriceau G, Hugo W, Hong A, et al. Tunable-combinatorial mechanisms of acquired resistance limit the efficacy of BRAF/MEK cotargeting but result in melanoma drug addiction. Cancer Cell 2015;27(2):240–256; doi: 10.1016/j.ccell.2014.11.018
41. Cohen SM, Mukerji R, Timmermann BN, et al. A novel combination of withaferin A and sorafenib shows synergistic efficacy against both papillary and anaplastic thyroid cancers. Am J Surg 2012;204(6):895–900; discussion 900–901; doi: 10.1016/j.amjsurg.2012.07.027
42. Choi YS, Kwon H, You MH, et al. Effects of dabrafenib and erlotinib combination treatment on anaplastic thyroid carcinoma. Endocr Relat Cancer 2022;29(6):307–319; doi: 10.1530/ERC-22-0022
43. Nucera C. A novel combined targeted therapy with bromodomain antagonist and MEK inhibitor in anaplastic thyroid cancer. Oncotarget 2019;10(7):686–687; doi: 10.18632/oncotarget.26591
44. Larkin J, Oya M, Martignoni M, et al. Avelumab plus axitinib as first-line therapy for advanced renal cell carcinoma: Long-term results from the JAVELIN renal 100 phase Ib trial. Oncologist 2023;28(4):333–340; doi: 10.1093/oncolo/oyac243
45. Chau V, Bilusic M. Pembrolizumab in combination with axitinib as first-line treatment for patients with renal cell carcinoma (RCC): Evidence to date. Cancer Manag Res 2020;12:7321–7330; doi: 10.2147/CMAR.S216605
46. Motzer RJ, Escudier B, Tomczak P, et al. Axitinib versus sorafenib as second-line treatment for advanced renal cell carcinoma: Overall survival analysis and updated results from a randomised phase 3 trial. Lancet Oncol 2013;14(6):552–562; doi: 10.1016/S1470-2045(13)70093-7
47. Ueda K, Suekane S, Hirano T, et al. Efficacy of axitinib as second-line treatment in locally advanced and metastatic renal cell carcinoma. Anticancer Res 2018;38(9):5387–5392; doi: 10.21873/anticanres.12868
48. Swiecicki PL, Bellile EL, Brummel CV, et al. Efficacy of axitinib in metastatic head and neck cancer with novel radiographic response criteria. Cancer 2021;127(2):219–228; doi: 10.1002/cncr.33226

49. Locati LD, Licitra L, Agate L, et al. Treatment of advanced thyroid cancer with axitinib: Phase 2 study with pharmacokinetic/pharmacodynamic and quality-of-life assessments. Cancer 2014;120(17):2694–2703; doi: 10.1002/cncr.28766
50. Cabanillas ME, Takahashi S. Managing the adverse events associated with lenvatinib therapy in radioiodine-refractory differentiated thyroid cancer. Semin Oncol 2019;46(1):57–64; doi: 10.1053/j.seminoncol.2018.11.004
51. Wagenaar TR, Ma L, Roscoe B, et al. Resistance to vemurafenib resulting from a novel mutation in the $BRAF^{V600E}$ kinase domain. Pigment Cell Melanoma Res 2014;27(1):124–133; doi: 10.1111/pcmr.12171
52. Danysh BP, Rieger EY, Sinha DK, et al. Long-term vemurafenib treatment drives inhibitor resistance through a spontaneous KRAS G12D mutation in a BRAF V600E papillary thyroid carcinoma model. Oncotarget 2016;7(21):30907–30923; doi: 10.18632/oncotarget.9023
53. Romano E, Pradervand S, Paillusson A, et al. Identification of multiple mechanisms of resistance to vemurafenib in a patient with $BRAF^{V600E}$-mutated cutaneous melanoma successfully rechallenged after progression. Clin Cancer Res 2013;19(20):5749–5757; doi: 10.1158/1078-0432.CCR-13-0661
54. Montero-Conde C, Ruiz-Llorente S, Dominguez JM, et al. Relief of feedback inhibition of HER3 transcription by RAF and MEK inhibitors attenuates their antitumor effects in BRAF-mutant thyroid carcinomas. Cancer Discov 2013;3(5):520–533; doi: 10.1158/2159-8290.CD-12-0531
55. Morelli MB, Amantini C, Santoni M, et al. Axitinib induces DNA damage response leading to senescence, mitotic catastrophe, and increased NK cell recognition in human renal carcinoma cells. Oncotarget 2015;6(34):36245–36259; doi: 10.18632/oncotarget.5768
56. Oktay K, Buyuk E, Oktem O, et al. The c-Jun N-terminal kinase JNK functions upstream of Aurora B to promote entry into mitosis. Cell Cycle 2008;7(4):533–541; doi: 10.4161/cc.7.4.5660
57. Bruner JK, Ma HS, Li L, et al. Adaptation to TKI treatment reactivates ERK signaling in tyrosine kinase-driven leukemias and other malignancies. Cancer Res 2017;77(20):5554–5563; doi: 10.1158/0008-5472.CAN-16-2593
58. Ku BM, Heo JY, Kim J, et al. ERK inhibitor ASN007 effectively overcomes acquired resistance to EGFR inhibitor in non-small cell lung cancer. Invest New Drugs 2022;40(2):265–273; doi: 10.1007/s10637-021-01121-6
59. Lohmeyer J, Nerreter T, Dotterweich J, et al. Sorafenib paradoxically activates the RAS/RAF/ERK pathway in polyclonal human NK cells during expansion and thereby enhances effector functions in a dose- and time-dependent manner. Clin Exp Immunol 2018;193(1):64–72; doi: 10.1111/cei.13128

Address correspondence to:
Chandrayee Ghosh, PhD
Department of Surgery
Stanford University
Center for Clinical Sciences Research (CCSR)
Room 3100, 269 Campus Dr
Stanford CA 94305
USA

E-mail: cghosh@stanford.edu